

## Ultrafast Electron Dynamics at Cu(111): Response of an Electron Gas to Optical Excitation

T. Hertel, E. Knoesel, M. Wolf, and G. Ertl

*Fritz-Haber-Institut der MPG, Faradayweg 4-6, D-14195 Berlin, Germany*

(Received 11 July 1995)

Time-resolved two-photon photoemission is used to directly investigate the electron dynamics at a Cu(111) surface with 60 fs laser pulses. We find that the time evolution of the photoexcited electron population in the first image state can be described only by solving the optical Bloch equations to properly account for coherence in the excitation process. Our experiments also provide evidence that the dynamics of photoexcited bulk electrons is strongly influenced by hot electron cascades and that the *initial* relaxation rates are in agreement with Fermi liquid theory.

PACS numbers: 78.47.+p, 73.25.+i

Ultrafast lasers have been extensively used to study the relaxation and recombination dynamics of excited bulk carriers in semiconductors [1–3] and nonequilibrium processes in laser-heated metals [4,5]. In contrast to techniques based on dynamic changes of macroscopic optical constants (e.g., transmission, reflection) time-resolved photoemission (TRPE) allows a *direct* measurement of the temporal evolution of the photoexcited electron distribution. In metals, where the initial relaxation dynamics is governed by ultrafast electron-electron (*e-e*) scattering, TRPE experiments have shown that complete thermalization of the nascent hot electrons to a Fermi distribution occurs on a time scale comparable to the electron-phonon (*e-ph*) relaxation time ( $\sim 1$  ps) [5]. Image-potential states at metal surfaces provide an ideal system to study an excited electron gas and its coupling to a continuum of substrate excitations [6,7]. Time-resolved studies of the image state dynamics, however, provide a challenge due to the fast decay of the excitation on the order of few to tens of femtoseconds depending on their binding energy with respect to the bulk band structure.

For coherent excitation of an electron gas with nearly transform limited laser pulses the rate of excitation is no longer given by Fermi's golden rule and cannot be described by simple rate equations. In order to properly account for coherent excitation as well as for energy relaxation and dephasing the optical Bloch equations must be solved [8]. This treatment reveals that the rate of excitation is *not* the highest when the field strength of the laser pulse reaches its maximum but rather when the pulse intensity decreases again. In this Letter we show that a precise measurement of the delay between the time profile of the pulse and the evolution of the excited state population, which critically depends on the energy relaxation time ( $T_1$ ), allows us to analyze lifetimes which are considerably shorter than the laser pulse duration.

We use time-resolved two-photon photoemission (2PPE) to investigate the response of an electron gas to femtosecond excitation at *low* excitation densities. Our experiments show that the transient population of photoexcited electrons in the ( $n = 1$ ) image state on

Cu(111) is retarded by  $\sim 17$  fs with respect to the time response of a two-photon process from the occupied surface state via a virtual intermediate state in the *sp*-band gap. The observed response can be successfully modeled employing the optical Bloch equations, while a simple (incoherent) rate equation model is inconsistent with the observed linewidth. Thereby, lifetimes ( $\tau_{n=1} = 10 \pm 3$  fs) considerably shorter than the laser pulse duration can be analyzed. We further provide evidence that the relaxation dynamics of photoexcited bulk electrons is strongly influenced by cascade processes via hot electron scattering with the cold Fermi sea, while the *initial* energy dependent relaxation rates agree with predictions from Fermi liquid theory.

The experiments were performed with a 200 kHz Ti:sapphire-seeded regenerative amplifier pumping an optical parametric amplifier (OPA) which outputs femtosecond pulses tunable from 470 to 730 nm [9]. The OPA output is compressed to 60 fs pulse duration and a thin (200  $\mu\text{m}$ ) beta barium borate crystal is used to generate second harmonic (UV) light. The UV and the visible beam are delayed with respect to each other and overlapped on the sample at  $45^\circ$  incidence angle polarized within the plane of incidence. The cross-correlation width between the visible and UV pulses is 90 fs measured directly at the sample. We use a low fluence of  $\sim 30 \mu\text{J}/\text{cm}^2$  in both arms to avoid space charge broadening and to keep the rise of the electronic temperature very small ( $\Delta T_e < 75$  K). Thus our experiment probes exclusively the nonequilibrated part of the electron distribution which has *not* thermalized to a Fermi distribution, in contrast to previous studies of laser-heated metals [4,5]. The Cu(111) crystal is mounted and cleaned in a UHV chamber as described elsewhere [10]. For some experiments the surface was exposed to CO at 90 K until the work function decreased by 0.2 eV resulting in complete quenching of surface and image states. The photoemitted electrons are detected within  $\pm 3^\circ$  along the surface normal using the time-of-flight technique.

The electronic structure of the Cu(111) surface exhibits an occupied surface state in the *sp*-band gap with a

binding energy of 0.45 eV (at 90 K) for zero parallel momentum ( $k_{\parallel} = 0$ ) [11]. A schematic energy diagram is shown in the inset of Fig. 1. The first ( $n = 1$ ) image state is located close to the upper edge of the  $sp$ -band gap at 4.1 eV above  $E_F$  [7]. Because its wave function penetrates deeply into the crystal, the image state is strongly coupled to electron-hole pair excitations in the bulk. Figure 1 (right panel) shows a 2PPE spectrum recorded with  $2\hbar\omega = 4.2$  eV pump and  $\hbar\omega = 2.1$  eV probe pulses in normal emission. The two features arise from the occupied surface state and the normally unoccupied ( $n = 1$ ) image state, respectively. Due to the lack of intermediate states in the band gap, photoemission from the surface state at  $k_{\parallel} = 0$  is a *nonresonant* two-photon process via a virtual state (see inset). The ( $n = 1$ ) image state can only be populated by electrons from states with  $k_{\parallel} \neq 0$ . The left panel shows the respective cross-correlation signals from the surface state and the ( $n = 1$ ) image state as a function of the delay between the UV pump and the visible probe. The full width at half maximum of the image state correlation trace (97 fs) is only slightly broader compared with the surface state (91 fs). However, the center of gravity of the image state correlation trace is clearly shifted by  $\Delta\tau = 17$  fs with respect to the surface state response towards delays where the UV pump pulse precedes the visible probe. This shift of  $\Delta\tau = 17 \pm 5$  fs has been observed for various pump energies between 4.2 and 4.7 eV. The observed

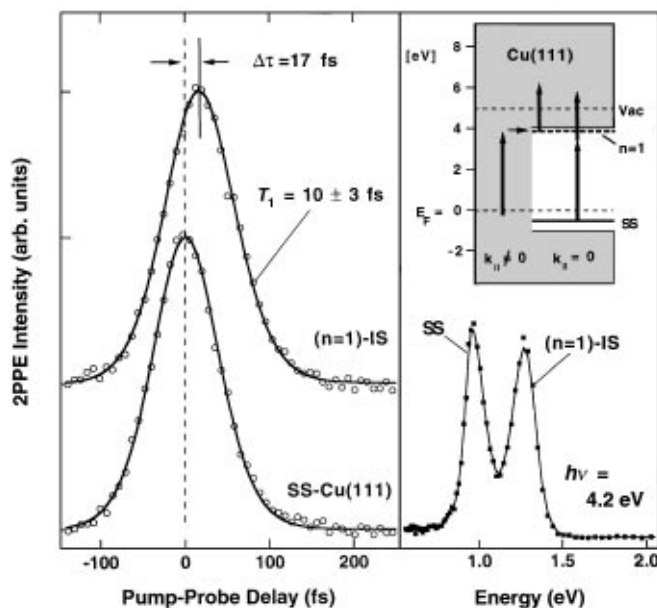


FIG. 1. Right panel: 2PPE spectrum from Cu(111) obtained with 4.2 eV pump and 2.1 eV probe pulses. The two features arise from the occupied surface state (SS) and the normally unoccupied ( $n = 1$ ) image state (IS), respectively. A schematic energy diagram of the electronic structure is shown in the inset (gray: projected bulk continuum). Left panel: Cross-correlation traces obtained for the SS and IS, respectively.

shift must be a consequence of the excitation process itself and is attributed to the different time response when a virtual state or a state with a finite lifetime serves as an intermediate in the 2PPE process. It cannot be attributed to the scattering time from bulk states at  $k_{\parallel} \neq 0$  to the center of the image state band because photoexcited electrons at 4.2 eV above  $E_F$  will relax on a time scale of less than 1 fs (see below).

For interpretation of the observed time response we model the 2PPE process by two sequential excitation steps. The first of these steps corresponds to the excitation from the ground state  $|1\rangle$  to the intermediate state  $|2\rangle$  with a transition frequency  $\omega_{12}$  (see Fig. 2). The second step corresponds to excitation to the final state  $|3\rangle$  where the electron is photoemitted from the surface. Since the time response of the *final* state population is not of relevance, we can restrict the discussion to a simple two level system consisting of  $|1\rangle$  and  $|2\rangle$ . The response to a time dependent optical perturbation  $\varepsilon(t) \cos(\omega t)$  is then described by the optical Bloch equations in the dipole and rotating frame approximations [8]:

$$\begin{aligned} \frac{d\rho_{22}}{dt} &= \frac{\mu_{12}\varepsilon(t)}{2i\hbar}(\tilde{\rho}_{12} - \tilde{\rho}_{21}) - \frac{\rho_{22}}{T_1} \\ \frac{d\tilde{\rho}_{12}}{dt} &= \frac{\mu_{12}\varepsilon(t)}{2i\hbar}(\rho_{22} - \rho_{11}) \\ &+ \left(i(\omega_{12} - \omega) - \frac{1}{T_2}\right)\tilde{\rho}_{12}, \end{aligned} \quad (1)$$

with  $\tilde{\rho}_{12} = \rho_{12} \exp[-i(\omega_{12} - \omega)t]$ , where  $\rho_{ij}$  are the density matrix elements,  $\mu_{12}$  is the transition dipole moment, and  $\varepsilon(t)$  is the envelope of the pump pulse. Here,  $T_1$  is the energy relaxation time and  $T_2 = (1/2T_1 + 1/T_2^*)^{-1}$  is the dephasing time in state  $|2\rangle$ , where  $T_2^*$

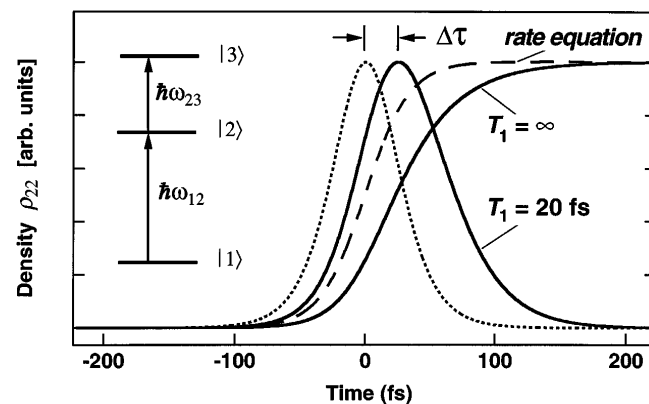


FIG. 2. Solution of the optical Bloch equations for the density  $\rho_{22}$  in the intermediate state  $|2\rangle$  of a three level system (see inset). Solid lines refer to solutions for resonant excitation ( $\omega = \omega_{12}$ ), while the dashed line is the time integrated pulse envelope (rate equation limit). For nonresonance excitation ( $\omega_{12} - \omega = 10\Gamma$ )  $\rho_{22}$  directly follows the time profile of the pulse (dotted line). All curves are normalized to the same maximum height.

accounts for “true” dephasing, e.g., by elastic scattering. Because  $T_2$  is related to the intrinsic linewidth  $\Gamma$  by  $\Gamma = 2/T_2$ , it is obvious that  $T_2$  cannot vanish for a transition with a finite linewidth as observed for the image states. However, the frequently used rate equation approach is only valid in the limit  $T_2 \rightarrow 0$  where it becomes equivalent to the optical Bloch equations [8]. Our discussion is restricted to small field strength with  $\int_{-\infty}^{\infty} [\mu_{12}\varepsilon(t)/\hbar] dt \ll \pi$ , which is satisfied for the low fluence used in the experiment. Figure 2 displays solutions of the Bloch equations for the excited state population  $\rho_{22}$  calculated for coherent resonant excitation ( $\omega = \omega_{12}$ ,  $T_2 = 2T_1$ ) with 60 fs sech<sup>2</sup>-shaped laser pulses (solid lines). The failure of a simple rate equation model employing Fermi’s golden rule to describe the time response for *coherent* excitation is seen most clearly by comparison of the solution of Eq. (1) (solid line,  $T_1 = \infty$ ) and the time integral of the pulse envelope (dashed line,  $T_1 = \infty$ ,  $T_2 = 0$ ). The latter would imply that the rate of excitation is proportional to the pulse intensity. However, the solution of the optical Bloch equations (for  $T_2 = 2T_1$ ) shows that the *rate* of excitation reaches its maximum (point of inflection) at times where the pump pulse (dotted line) has already passed its maximum. It is precisely this delay which enhances our sensitivity to the intermediate state lifetime. For example, for a lifetime  $T_1 = 20$  fs and  $T_2 = 2T_1$  the maximum in the excited state population is shifted by  $\Delta\tau = 27$  fs as seen by comparison with the dotted line in Fig. 2. On the other hand, if the frequency of the perturbation  $\omega$  is tuned out of resonance ( $\omega_{12} - \omega = 10\Gamma$ ),  $\rho_{22}$  follows directly the time profile of the pulse (dotted line). The nonresonant 2PPE process from the surface state allows, therefore, one to determine the true time zero of the pump pulse with respect to the probe. Since the measured signal is proportional to the time integrated population in the final state  $|3\rangle$ , the second photoemission step can be treated by convoluting the calculated population  $\rho_{22}$  with the probe pulse.

For data analysis the pulse width and time zero were first determined from the correlation trace of the surface state (Fig. 1) for the nonresonant transition ( $\omega_{12} - \omega = 4\Gamma$ ). The measured trace of the ( $n = 1$ ) image state is then fitted by a correlation trace calculated for resonant coherent excitation ( $T_2 = 2T_1$ ) with the relaxation time  $T_1$  as free parameter. From this analysis we obtain a lifetime  $T_1 = 10 \pm 3$  fs for the ( $n = 1$ ) image state on Cu(111). If the measured linewidth of 85 meV derived from 2PPE spectra [7] is included in the analysis ( $T_2 = 2/\Gamma$ ), we obtain a lower limit for the true dephasing time of  $T_2^* \gg 30$  fs. We note that a simple rate equation model (i.e., assuming  $T_2 \sim 0$ ) would yield  $T_1 = 20$  fs, but the latter model would imply an infinitely broad linewidth, in clear contrast to the experiment. Thus by employing the optical Bloch equations we are able to analyze lifetimes considerably shorter than the laser pulse duration. This would not be possible without a

precise measurement of the true time zero employing the nonresonant two-photon process from the surface state as a reference.

Schoenlein *et al.* have studied the image state dynamics on silver surfaces with TRPE [6]. On Ag(111) the first image state lies close to the band edge and is very short lived, similar to Cu(111). However, the latter experiment failed to resolve the image state lifetime because only changes in the cross-correlation *width* were analyzed [6]. Image state lifetimes on Cu(111) have also been deduced indirectly from linewidth measurements which revealed a lifetime broadening  $\Gamma = 85 \pm 10$  meV [7]. This corresponds to a lifetime  $\tau = \hbar/\Gamma$  of  $8 \pm 1$  fs, which is in nice agreement with our direct measurement.

The analysis employing the optical Bloch equations provides a basis to extend our studies to the more complicated hot electron dynamics in the bulk. Figure 3 displays the time resolved 2PPE signal from photoexcited hot electrons at different energies above  $E_F$  obtained by cross-correlating 2.23 eV (visible) and 4.45 eV (UV) laser pulses with 65 fs duration. In order to eliminate contributions due to surface and image states the surface was exposed to CO at 90 K. Identical findings for the electron relaxation were obtained for  $0.5 \leq E - E_F \leq 1.3$  eV on clean Cu(111). The zero time delay was determined on the clean surface employing the 2PPE signal from the surface state, as discussed above. All

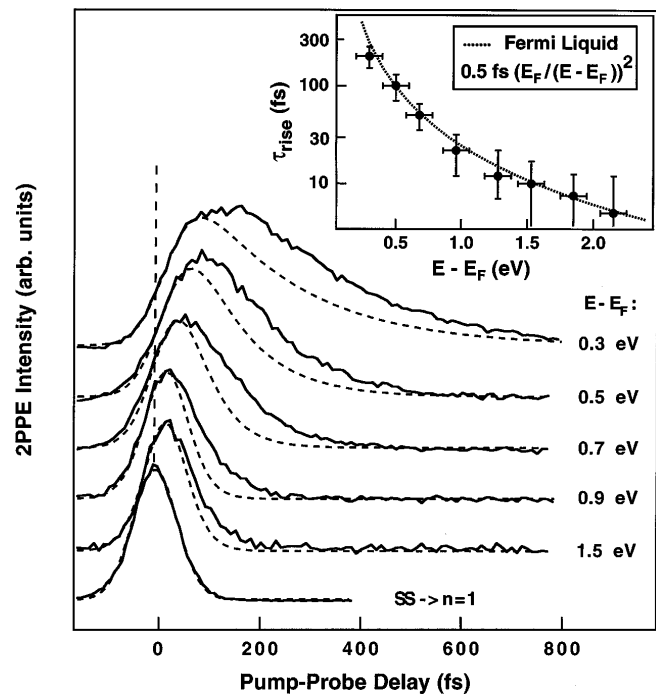


FIG. 3. 2PPE of photoexcited electrons for different energies relative to  $E_F$  vs time delay between the 2.23 eV pump and 4.45 eV probe pulse. Analysis of the initial rise using the optical Bloch equations (dashed lines) yields lifetimes  $\tau_{\text{rise}}$  (●) in agreement with Fermi liquid theory (see inset).

correlation traces reveal an asymmetry in time indicating that the signal arises predominately from processes where the visible pulse acts as a pump while the UV pulse serves as a probe. Furthermore, the relaxation dynamics becomes obviously slower for energies close to  $E_F$ , where the photoemission signal persists for several hundred femtoseconds.

The relaxation of the photogenerated nonequilibrium electron distribution is a complicated many-body problem. According to Landau's Fermi liquid theory the lifetime of an excited electron  $\tau_{e-e}$  is determined by the available phase space between the electron energy  $E$  and the Fermi level  $E_F$  and is given by  $\tau_{e-e} = \tau_0[E_F/(E - E_F)]^2$  with  $\tau_0 = 128/\pi^2\sqrt{3}\omega_p$  [12]. For copper the plasmon frequency is  $\omega_p \sim 10$  eV yielding  $\tau_0 = 0.5$  fs [13]. On the average electrons will halve their energy per scattering event and thereby excite electrons from below  $E_F$  into unoccupied states above the Fermi level. As a consequence, secondary electrons originating from these scattering processes will populate states with  $E - E_F < \hbar\omega$ . The time evolution of the electron distribution is, therefore, not only determined by the decay (loss) of the initial photoexcited electron distribution but also by cascade processes (gain) from secondary electrons.

Our data analysis shows that the correlation traces in Fig. 3 *cannot* be satisfactorily described by a model which considers only depletion of the initial photoexcited population. Either the rise or the decay of the signal cannot be modeled simultaneously with a single relaxation time at each energy. We have, therefore, analyzed the initial rise of the signal using the Bloch equations (dashed lines) because at early times the dynamics should be less affected by cascade processes. We assume rapid dephasing ( $T_2 \ll 2T_1$ ) because momentum conservation implies that photoexcitation within the copper *sp* band evolves indirect transitions, which destroys the coherence of the excitation. While the initial rise can be satisfactorily reproduced, a contribution to the signal persisting to longer time delays cannot be described by the decay of the initial population with a single relaxation time (dashed lines in Fig. 3). This effect becomes more pronounced for energies closer to  $E_F$ , and we take this as evidence that the dynamics of photoexcited bulk electrons is strongly influenced by cascade processes. Furthermore, a fraction of the initial electron distribution will be lost by transport out of the detection volume into the bulk [14]. The *decay* of the cross-correlation signal is, therefore, governed by a complicated superposition of the energy dependent lifetime in each state, cascade, and transport process.

Our analysis of the *initial rise* of the correlation data minimizes interference with cascade and transport effects and allows us to estimate hot electron lifetimes as a function of the energy above  $E_F$ . The resulting relaxation times  $\tau_{\text{rise}}$  are compared with the prediction from Fermi liquid theory in the inset of Fig. 3. The agreement

between the experimentally obtained  $\tau_{\text{rise}}$  and Fermi liquid theory is surprisingly good taking into account that the electronic structure of copper deviates from an ideal free electron gas. Since the Cu *3d* bands lie 2 eV below  $E_F$ , copper may still be regarded as a nearly free electron metal in the energy range probed by our experiment. Other TRPE studies have reported lifetimes  $\sim 2.5$  times longer than predicted by Fermi liquid theory [5,14]. However, in these experiments only the decay of the electron distribution was analyzed which is, as we have shown, affected by cascade processes.

In conclusion, we have presented experimental evidence that, for coherent excitation of an electron gas by nearly transform limited laser pulses, excited state lifetimes—considerably shorter than the pulse duration—can be determined if the precise time zero of the exciting laser pulse is known. The sensitivity to the excited state lifetime is due to a delay in the *rate* of excitation with respect to the temporal profile of the pump pulse. This effect can be readily accounted for by the optical Bloch equations.

We acknowledge valuable comments by M. Aeschlimann, R. Haight, P. Saalfrank, and inspiring discussions with I. V. Hertel on Bloch's equations.

- 
- [1] J. Shah, *Solid State Commun.* **32**, 1051 (1989).
  - [2] J. R. Goldman and J. A. Prybyla, *Phys. Rev. Lett.* **72**, 1364 (1994).
  - [3] A. Leitenstorfer, A. Lohner, T. Elsaesser, S. Haas, F. Rossi, T. Kuhn, W. Klein, G. Boehm, G. Traenkle, and G. Weimann, *Phys. Rev. Lett.* **73**, 1687 (1994).
  - [4] R. W. Schoenlein, W. Z. Lin, J. G. Fujimoto, and G. L. Eesley, *Phys. Rev. Lett.* **58**, 1680 (1987).
  - [5] W. S. Fann, R. Storz, H. W. K. Tom, and J. Bokor, *Phys. Rev. Lett.* **68**, 2834 (1992); *Phys. Rev. B* **46**, 13592 (1992).
  - [6] R. W. Schoenlein, J. G. Fujimoto, G. L. Eesley, and T. W. Capehart, *Phys. Rev. B* **43**, 4688 (1991).
  - [7] T. Fauster and W. Steinmann, in *Electromagnetic Waves: Recent Development in Research*, edited by P. Halevi (Elsevier, Amsterdam, 1995).
  - [8] R. Loudon, *The Quantum Theory of Light* (Oxford University Press, New York, 1983).
  - [9] M. K. Reed, M. S. Armas, M. K. Steiner-Shepard, and D. K. Negus, *Opt. Lett.* **20**, 605 (1995).
  - [10] T. Hertel, E. Knoesel, E. Hasselbrink, M. Wolf, and G. Ertl, *Surf. Sci.* **317**, L1147 (1994).
  - [11] R. Pagiago, R. Matzdorf, and A. Goldmann, *Surf. Sci.* **336**, 113 (1995), and references therein.
  - [12] D. Pine and P. Nozieres, *The Theory of Quantum Liquids* (Benjamin, New York, 1966).
  - [13] N. W. Ashcroft and N. D. Mermin, *Solid State Physics* (Saunders College, Philadelphia, 1988).
  - [14] C. A. Schmuttenmaer, M. Aeschlimann, H. E. Elsayed-Ali, R. J. D. Miller, D. A. Mantell, J. Cao, and Y. Gao, *Phys. Rev. B* **50**, 8957 (1994).